Available online at www.sciencedirect.com
ScienceDirect
Geochimica et Cosmochimica Acta 72 (2008) 5885–5895
Geochimica et Cosmochimica Acta
www.elsevier.com/locate/gca

Cd adsorption onto *Pseudomonas putida* in the presence and absence of extracellular polymeric substances

Masato Ueshima, Brian R. Ginn, Elizabeth A. Haack, Jennifer E.S. Szymanowski, Jeremy B. Fein *

Department of Civil Engineering and Geological Sciences, University of Notre Dame, Notre Dame, IN 46556, USA

Received 28 April 2008; accepted in revised form 18 September 2008; available online 25 September 2008

Abstract

The role of bacterial extracellular polymeric substances (EPS) in metal adsorption was determined by studying Cd adsorption onto the gram-negative bacterial species *Pseudomonas putida* with and without enzymatic removal of EPS from the biomass material. A range of experimental approaches were used to characterize the Cd adsorption reactions, including bulk proton and Cd adsorption measurements, FTIR spectroscopy, and fluorescence microscopy. The proton-reactivities of the biomass samples with EPS are not significantly different from those obtained for EPS-free biomass. Similarly, the presence of EPS does not significantly affect the extent of Cd removal from solution by the biomass on a mass-normalized basis, based on bulk Cd adsorption measurements conducted as a function of pH, nor does it appear to strongly affect the Cd-binding groups as observed by FTIR. However, fluorescence microscopy indicates that Cd, although concentrated on cell walls, is also bound to some extent to EPS. Together, the results from this study suggest that the *P. putida* EPS can bind significant concentrations of Cd from solution, and that the nature and mass-normalized extent of the binding is similar to that of the cell wall. Therefore, the EPS-bearing systems do not exhibit enhanced mass-normalized removal of Cd from solution relative to the EPS-free systems. The presence of the EPS effectively increases the viability of cells exposed to aqueous Cd, likely due to sequestration of the Cd away from the cells due to Cd-EPS binding.

1 INTRODUCTION

Complexation of aqueous metal cations onto bacterial cell walls and onto biofilm material in general can control the mobility, speciation and bioavailability of metals. Most previous studies of proton and metal adsorption onto bacterial biomass have involved cells with little or no extracellular polymeric substance (EPS) material present. However, most bacteria in geologic systems exist predominantly in biofilms that are attached to mineral surfaces. Biofilms are an attached growth state of bacteria where structured communities of cells are linked together in a matrix that includes secreted extracellular polysaccharides, proteins, lipids, and DNA (Costerton et al., 1995; Davey and O'Toole, 2000; Flemming and Wingender, 2001; Allesen-Holm et al., 2006), and this EPS-rich matrix also aids the adhesion of biofilms to mineral surfaces (Beveridge, 1988). EPS consists of glucose, fructose, mannose, pyruvate and fucose, and mannuronic- and guluronic-acid complexes (Brisou, 1995). Isolation of EPS in sufficient quantities to conduct metal adsorption experiments is difficult. In this study, we examine the effect of the EPS on Cd binding by comparing Cd adsorption behaviors of biomass which has had EPS molecules left intact to that which has had the EPS molecules enzymatically removed.

The EPS molecules of most bacterial species are negatively charged under circumneutral pH conditions due to the presence of predominantly carboxylic and phosphoryl functional groups (Beveridge, 1988). A large number of experimental studies have examined metal-EPS binding reactions over the past twenty years (e.g., Mittelman and Geesey, 1985; Ferris et al., 1989; Geesey and Jang, 1990;

* Corresponding author. Fax: +1 574 631 9236.
E-mail address: fein@nd.edu (J.B. Fein).

0016-7037/$ - see front matter © 2008 Elsevier Ltd. All rights reserved.
doi:10.1016/j.gca.2008.09.014

McLean et al., 1990; Vincent et al., 1994; Foster et al., 2000; Lau et al., 2005; Comte et al., 2006a,b; Guibaud et al., 2006). Although EPS can clearly adsorb significant concentrations of a wide range of metals and thereby affect metal budgets in aqueous systems, the importance of metal-EPS binding relative to metal-cell wall binding remains undetermined. XAS and X-ray standing waves have been used to study the relative sorption of Pb to biofilms (as a whole) on alumina surfaces (Templeton et al., 2001, 2003), demonstrating the importance of both sorbents in controlling Pb speciation. A more recent study of Zn adsorption to Gram-negative bacteria with intact EPS (Guine et al., 2006) used potentiometric titrations, modeling, and XAS to demonstrate that more Zn is adsorbed than would be predicted by available sites on the bacterial cell wall alone, suggesting that EPS sorption of Zn can significantly affect the overall adsorption of Zn by the biofilm. Toner et al. (2005) used XAS to demonstrate the importance of phosphoryl and carboxyl binding sites for Zn in a bacterial biofilm under pH 7 conditions. Liu and Fang (2002) have conducted the only potentiometric titrations of isolated EPS molecules, documenting significant buffering capacity over a broad pH range, with site concentrations in excess of those found on bacterial cells on a per gram basis. These results are consistent with the findings of Tourney et al. (2008) who document slightly higher proton-active site concentrations in biofilms with intact EPS relative to those with EPS removed.

In order to determine the role and relative importance of proton and metal binding onto EPS molecules compared with binding onto bacterial cell walls, we prepared two types of bacterial biomass samples: one with EPS intact and the other with EPS removed using an enzyme, glucoamylase, that cuts α-glucosidic bonds (Zherebtsov et al., 1995). We conducted potentiometric titrations to compare the concentrations of proton-active binding sites within the two types of biomass samples. We also conducted titrations to compare the proton reactivity of biomass grown using liquid media to that grown using solid media to determine if the growth environment influences the reactivity of the EPS. In addition, we measured Cd adsorption onto these two types of bacterial samples as a function of pH with a fixed concentration of Cd in solution. The FTIR spectra of the Cd-adsorbed bacterial samples were measured in order to help identify the functional groups responsible for Cd binding and to compare binding environments in the EPS-bearing and EPS-free samples. In addition, the spatial distribution of Cd near and on bacterial cells with intact EPS was visualized using fluorescence microscopy, and we conducted cell viability tests for bacteria with and without EPS, in the presence and absence of Cd, in order to ascertain the effect of EPS on Cd toxicity to the cells.

2. MATERIAL AND METHODS

2.1. Biomass growth

Cells and EPS of *Pseudomonas putida*, an aerobic Gram-negative bacterial species, were produced by initially culturing the bacteria for 24 h in a modified M9 medium (6.78 g/L Na_2PO_4, 3 g/L KH_2PO_4, 0.5 g/L NaCl, 0.1 mM $CaCl_2{\cdot}2H_2O$, 1 mM $MgSO_4{\cdot}7H_2O$, 0.3% glucose, 0.03 g/L $NaNO_3$) with a pH of approximately 7. After 24 h of growth, the biomass contained a significant amount of EPS. Bacterial cells with intact EPS were removed from the nutrient medium by centrifugation and rinsed three times with sterilized 0.1 M $NaClO_4$ (the electrolyte used in the experiments). Although we have not conducted characterization studies of the EPS molecules in this study, under these growth conditions, *Pseudomonas putida* produces mainly alginate-like polysaccharides, consistent in their composition of mannuronic and guluronic acids (Conti et al., 1994). In this study, biomass is described in terms of wet mass, determined by centrifugation at 5800*g* for 60 min, and corresponds to approximately five times the dry mass of the cells (Borrok and Fein, 2005).

2.2. Enzyme treatments

Polysaccharides such as alginate can be degraded through an enzyme treatment (e.g., Böckelman et al., 2003; Brisou, 1995; Sutherland, 1995; Conti et al., 1994). The enzyme glucoamylase is effective at breaking the α-1,4-glucosidic bonds within alginate (Zherebtsov et al., 1995), and therefore we used glucoamylase to remove the EPS molecules from the *P. putida* cells in our washed cultures. Approximately 0.5 g of bacterial biomass (wet mass) was suspended in fifty units of glucoamylase (Fisher, analytical grade) and 50 mL of 0.1 M $NaClO_4$. The suspensions were shaken in an incubator for 2 h at 32 °C. The suspensions were then centrifuged and rinsed three times with sterilized 0.1 M $NaClO_4$. Untreated and enzyme-treated biomass samples were imaged using an environmental scanning electron microscope (ESEM) in order to determine the extent of EPS removal by the enzyme treatment. The imaging was conducted at 20 kV of acceleration voltage, 100–300 Pa of vacuum pressure, 20–80% humidity, and with a spot size of 350 nm.

2.3. Potentiometric titrations

Three types of potentiometric titrations were performed using 25–35 g/L (wet mass) suspensions of *P. putida* biomass in 0.1 M $NaClO_4$: (1) titrations using enzyme-treated biomass (EPS removed) grown in liquid media (described above); (2) titrations using untreated biomass (EPS intact) grown in liquid media; and (3) titrations using untreated biomass grown on solid media. The solid medium was a trypticase soy agar with 0.5% yeast extract added, and the biofilm that grew was removed by scraping with a heat sterilized microscope slide. The removed biomass was then washed following an identical procedure to that described above for the biomass grown in liquid media.

Ten titrations of each type were conducted, with biomass grown and washed separately for each titration. In each titration, the electrolyte solution was bubbled with N_2 gas for 1 h prior to use, and the titration cell containing the bacterial suspension was kept under a N_2 atmosphere during the experiment. Each suspension was continuously stirred with a small magnetic stir bar during the titration.

The titrations were first run down-pH with aliquots of 1.0005 N HCl to approximately pH 2.5, then up-pH with aliquots of 1.005 N NaOH to approximately pH 11, using an autotitrator assembly that measured pH after each incremental addition of acid or base. Each addition of acid or base occurred only after a pH electrode stability of 0.1 mV/s was attained. Although it is likely that the buffering capacity of the bacterial suspensions extend to extremely low pH conditions (e.g., Fein et al., 2005), we limited the potentiometric titrations to a low pH value of 2.5 in order to avoid excessive disruption of the Gram-negative cell wall structure (Borrok et al., 2004), although some disruption cannot be avoided if the low pH proton-activity of the cell wall functional groups are to be probed.

2.4. Cadmium adsorption experiments

Washed samples of either enzyme-treated or untreated biomass were suspended in high density polyethylene test tubes with a 0.1 M $NaClO_4$ electrolyte to form a suspension of 1.2 g/L of bacteria (wet mass). A parent solution of aqueous Cd in 0.1 M $NaClO_4$ was prepared from a commercially-supplied 1000 ppm Cd reference solution. The pH of this parent solution was adjusted to 5.9, and aliquots of this solution were added to the bacterial suspensions to achieve a final Cd concentration of 10 ppm, and topped off with additional 0.1 M $NaClO_4$. The pH of each test tube was adjusted to the desired value using small aliquots of 1 M HNO_3 or NaOH, and the systems were allowed to equilibrate for two hours. The Cd concentration and pH values studied were such that all solutions were undersaturated, and any removal of Cd from solution was caused only by adsorption of Cd onto biomass. Control experiments demonstrated that without biomass present, there was negligible removal of Cd from the bulk solution. Previous studies involving *Bacillus subtilis* have demonstrated that equilibrium of Cd adsorption reactions occurs in less than 1 h, and that the adsorption reactions are fully reversible (e.g., Fowle and Fein, 2000). In all experiments, pH was monitored every 30 min, and adjusted as required using minute aliquots of 1 M HNO_3 or NaOH. The final pH was measured after two hours, and the solution was then centrifuged and filtered through a 0.45 μm cellulose nitrate membrane. The filtered supernatant was analyzed for dissolved Cd using an inductively coupled plasma-optical emission spectroscopy technique with matrix-matched standards. The concentration of metal adsorbed to biomass in each vessel was calculated by subtracting the concentration of metal that remained in solution from the original Cd concentration in each experiment. The experiments were performed in triplicate, and the average pH and extent of Cd adsorption are calculated along with a standard deviation value for each parameter. The filtered residues from some of the pH 7.6 Cd-bearing systems were analyzed using fluorescence microscopy (FM) to visualize the Cd distribution between EPS and cells. The pH 7.6 residues were also analyzed using Fourier transform- infrared spectroscopy attenuated total reflectance (FTIR-ATR) microscopy in order to place constraints on the nature of Cd binding in each sample. FM and FTIR-ATR procedures are described below.

2.5. Fluorescence microscopy

The Cd distribution near the non-treated EPS-bearing bacterial surfaces was visualized using a combination of fluorescence indicators: Fluozin-1 to show the presence of Cd(II), and DAPI (4′6-diamidino-2-phenylindole) to fluoresce intracellular material in order to locate the cells spatially. The biomass (1.2 g wet mass/L) was suspended in a pH 7.6, 0.1 M $NaClO_4$ solution with 10 ppm Cd, and then filtered prior to examination with fluorescence microscopy. The green fluorescence images that were derived from Fluozin-1 treatment and the blue fluorescence images derived from DAPI treatment were combined using Adobe Photoshop CS. The DAPI counts, determined using fluorescence microscopy after a 1/5000 dilution, indicated that the 1.2 g/L bacterial suspension concentration corresponds to $(2.5 \pm 0.6) \times 10^8$ cells/mL.

2.6. Fourier transform infrared spectroscopy-attenuated total reflectance (FTIR-ATR) microscopy

FTIR-ATR microscopy (Böckelman et al., 2003) was used to elucidate the chemical binding environment of Cd in association with the untreated and enzyme-treated cells. Treated and untreated biomasses were analyzed before and after reaction with Cd in batch experiments, as described above. Following the batch experiments the cell solutions were centrifuged and the pastes were mounted on a glass slide. Analyses were performed in an open atmosphere using the IlluminatIR FTIR microscpectrometer with a diamond total attenuated reflectance (ATR) objective. FTIR spectra were collected from 400 to 4000 cm^{-1}. Background spectra of water and of the glass slide were collected prior to measurement of biomass samples. For each sample, 128 scans were signal averaged and a total of ten spectra were collected from different spots on the sample slide in order to evaluate the heterogeneity in the sample. FTIR spectra were post-processed using the Grams/32 AO (6.00) software from Galactic Industries (Thermo Electron Corporation, Madison, Wisconsin). Spectra were baseline corrected and were normalized to the height of the peak at 1240 cm^{-1} to account for differences in the thickness of the cells on the sample slide. Individual band intensities for bands associated with the biomass in the region 900–1800 cm^{-1} were determined using a non-linear least-squares peak-fitting algorithm. A combined Lorentzian/Gaussian lineshape was found to provide good results in all samples. Experimental data for organic molecules are often fit using Voigt (combined Lorentzian/Gaussian) lineshapes (e.g. Xu et al., 2000; Arroyo et al., 2005).

FTIR-ATR microscopy was run on four sets of samples: (1) untreated cells, (2) untreated cells exposed to 50 ppm Cd, (3) enzyme-treated cells and (4) enzyme-treated cells exposed to 50 ppm Cd. Because the samples were analyzed as wet (centrifuged) pastes, subtraction of water from the spectra made the region from 1450 to 600 cm^{-1} most useful in subsequent discussion of the collected spectra.

2.7. Cell viability tests

In order to understand the effects of EPS on Cd toxicity to the bacterial cells, we conducted cell viability tests at

pH 6.5, in 0.1 M $NaClO_4$. We measured cell viability in four systems: (1) Untreated cells with no Cd present; (2) Untreated cells with 10 ppm Cd present; (3) Enzyme-treated cells with no Cd present; and (4) Enzyme-treated cells with 10 ppm Cd present. In each case, the biomass suspension was shaken in a dark room at room temperature for 6 h. The pH of each batch experiment was adjusted to 6.5 using small volumes of NaOH or HNO_3. The viability of each sample was determined by using the LIVE/DEAD® *Bac*Light™ kit (Molecular Probes, Eugene OR). Briefly, cell suspensions were stained with two nucleic acid stains, SYTO® 9 (a green fluorescent stain) and propidium iodide (a red fluorescent stain). After exposure to these stains, live bacteria with intact membranes fluoresce green, while dead bacteria with damaged membranes fluoresce red when examined by fluorescence microscopy using the appropriate optical filters. We counted the number of green and red fluorescing cells at five locations within each biomass sample tested, and viability is expressed as the percentage of green cells averaged over the five locations in each sample.

3. RESULTS AND DISCUSSION

3.1. Effectiveness of enzyme treatment

The ESEM images of the glucoamylase-treated and untreated *Pseudomonas putida* biomass samples reveal the effectiveness of the enzyme in degrading and detaching extracellular materials from the bacterial cells (Fig. 1A and B). The untreated sample displays a cloudy material that completely covers the cells, indicating that there is extensive EPS growth in the biomass preparation, and that EPS still remains on the cells after the 0.1 M $NaClO_4$ wash procedure (Fig. 1A). Conversely, in the sample treated with glucoamylase, individual cells are visible, with minimal amounts of the cloudy material visible on the cells (Fig. 1B). These results clearly show that the glucoamylase treatment that we use effectively removes virtually all EPS material from the biomass samples, leaving intact EPS-free cells in the treated samples.

3.2. Potentiometric titration experiments

The three types of biomass studied here exhibited remarkably similar proton-active buffering behavior. Although it would be difficult to depict all of the titrations on one diagram, we compare typical titrations from each set of titrations in Fig. 2, and modeling results from all of the titrations are compiled in Table 1. Fig. 2 demonstrates that there is virtually no difference between the titrations of the enzyme-treated and the untreated biomass samples grown either in liquid or on solid media.

For clarity, Fig. 2 does not depict data from all ten titrations conducted using each biomass type, however, we can quantitatively compare these results using surface complexation modeling. We use a non-electrostatic approach to determine the number of types of binding sites that are required to account for the observed buffering behavior, and the concentration and acidity constant of each site type. Following the approach used by Fein et al. (2005) to model titration data for *B. subtilis*, we represent the surface site reactivity using discrete proton-active sites that deprotonate according to the following reaction stoichiometry:

$$\text{R-A}_i\text{H}^o = \text{R-A}_i^- + \text{H}^+ \tag{1}$$

where R-A_i represents a biomass surface functional group type and i is an integer $\geqslant 1$. The generalized mass action equation for the above reaction is:

$$K_{(i)} = \frac{[\text{R-A}_i^-]a_{\text{H}^+}}{[\text{R-A}_i\text{H}^o]} \tag{2}$$

where K and a represent the equilibrium constant and activity of the subscripted reaction or species, respectively, and where brackets represent the concentration of biomass sites in mol/L of solution. Each biomass site R-A_i represents a discrete site with its own site concentration and acidity constant. FITEQL (Westall, 1982) was used as the computational tool to determine the number of discrete sites necessary to account for the observed buffering behavior and to solve for the site concentrations and acidity constants for each type of site. Because we measured proton adsorption at only one ionic strength, we neglect the effects of the surface electric fields on the adsorption equilibria. For each model tested, FITEQL calculates a variance function, $V(\text{Y})$, that describes the goodness of fit of the model to the experimental measurements. The best fitting model was determined to be the one that yields the lowest $V(\text{Y})$ value and displays the best visual fit to the experimental data. Each titration was modeled separately.

A 4-site model, with a discrete deprotonation reaction associated with each site type, provides the best fit to the experimental data of all three types of biomass samples. Models using less than four site types yield significantly higher $V(\text{Y})$ values and exhibit a worse visual fit to the experimental data. Models utilizing more than four sites fail to converge, indicating that the titration behavior is overconstrained and cannot uniquely constrain the properties of more than four discrete sites. The best fitting averaged deprotonation constants and averaged site concentrations for the three types of biomass samples are compiled in Table 1, along with 1-sigma standard deviations for each of these values from the 10 titrations of each biomass type.

Table 1 demonstrates that, within experimental uncertainty, the proton-reactivities of the three different biomass samples are not significantly different from one another. This conclusion holds true for both the acidity constant values as well as for the site concentrations. Within the error of these measurements, the three biomass sample types behave identically, suggesting that either the EPS molecules exhibit no proton reactivity or that they exhibit an identical proton reactivity to that observed for the EPS-free cells. Table 1 also shows that the proton reactivity modeling parameters that we calculate for the three biomass sample types are within experimental uncertainties of corresponding values from the universal framework for modeling proton binding onto bacterial surfaces as determined by Borrok et al. (2005), who modeled titrations of 36 bacterial species and consortia.

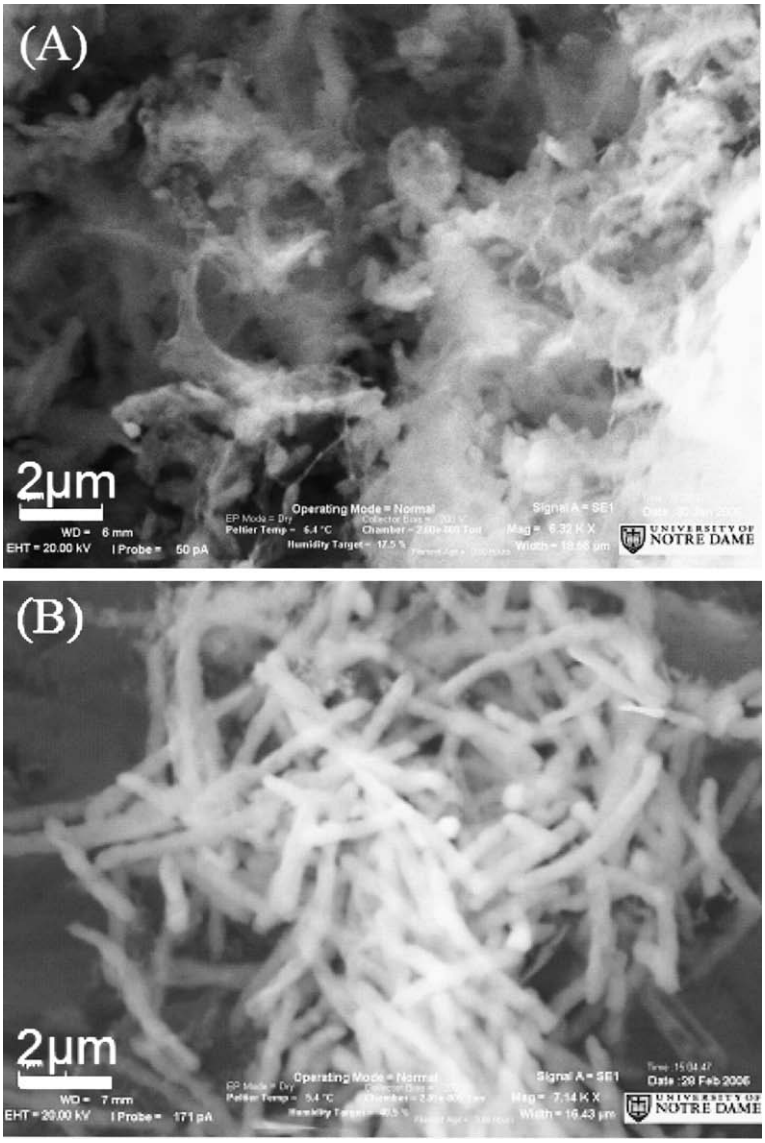

Fig. 1. Environmental scanning electron microscope images of (A) untreated and (B) enzyme-treated *Pseudomonas putida* biofilms.

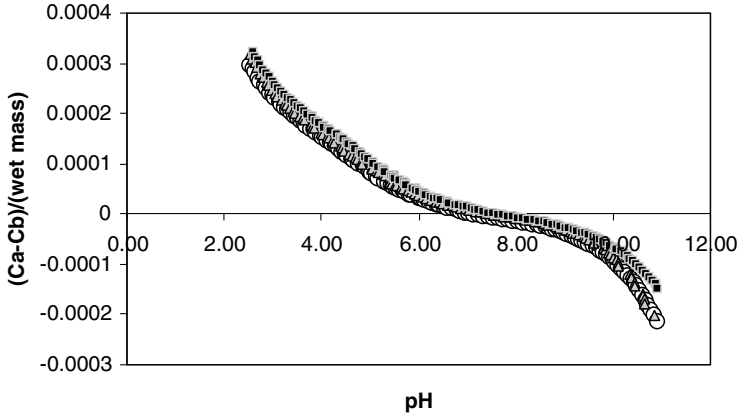

Fig. 2. Representative potentiometric titration data for *P. putida* (~30 g/L, wet wt.) biomass samples in 0.1 M $NaClO_4$. Open circles represent data from experiments using untreated (EPS-bearing) biomass; grey triangles represent data from experiments using enzyme-treated (EPS-free) biomass; black squares represent data from experiments using untreated (EPS-bearing) biomass grown on a solid agar medium.

Table 1
Comparison of modeling parameters

Biomass type	p*K*1	p*K*2	p*K*3	p*K*4	[Site 1][a]	[Site 2]	[Site 3]	[Site 4]
Untreated								
P. putida[b]	3.5 ± 0.2	5.0 ± 0.2	6.9 ± 0.4	10.1 ± 0.1	82 ± 18	105 ± 12	42 ± 7	128 ± 33
Enzyme-treated								
P. putida[c]	3.2 ± 0.5	4.7 ± 0.4	6.4 ± 0.6	9.8 ± 0.5	86 ± 11	99 ± 19	56 ± 23	119 ± 40
Agar-grown								
P. putida[d]	4.2 ± 1.1	4.6 ± 0.8	7.7 ± 0.5	10.5 ± 0.2	97 ± 11	114 ± 21	55 ± 16	207 ± 97
Borrok et al. (2005)[e]	3.1	4.7	6.6	9.0	110 ± 70	91 ± 38	53 ± 21	66 ± 30

[a] Site concentrations in μmol/gm wet mass.
[b] Averages and standard deviations from 10 titrations of untreated biomass samples in 0.1 M $NaClO_4$.
[c] Averages and standard deviations from 9 titrations of enzyme-treated biomass samples in 0.1 M $NaClO_4$.
[d] Averages and standard deviations from 5 titrations of untreated, agar-grown biomass samples in 0.1 M $NaClO_4$.
[e] Borrok et al. (2005) used fixed p*K* values and solved for site concentrations using 225 titration datasets from experiments involving 36 bacterial species and consortia.

3.3. Cd adsorption experiments

The results from the Cd adsorption experiments are illustrated in Fig. 3, which demonstrates that the extent of Cd adsorption onto the enzyme-treated biomass is identical, within experimental uncertainty, to that observed for the untreated biomass. Error bars on the data symbols within Fig. 3 represent 1-sigma uncertainties based on triplicate experiments under similar pH conditions. The presence of the EPS molecules in the untreated biomass samples does not significantly affect the extent of Cd adsorption that the samples exhibit relative to that observed for the enzyme-treated samples on a per gram basis. These Cd adsorption experimental results are consistent with the potentiometric titration results in that both sets of experiments suggest that either the EPS molecules exhibit no proton or metal-binding reactivity, or that the EPS molecules exhibit an identical proton and metal-binding reactivity to that observed for the EPS-free cells.

3.4. Spatial distribution of Cd in biomass samples

In order to distinguish between the two possible explanations for the proton and Cd adsorption results, we examined the spatial distribution of Cd on or near the bacterial cells using fluorescence microscopy. The results of fluorescence microscopy using DAPI and Fluozin-1 stains of an untreated biomass sample with intact EPS are shown in Fig. 4. We used the DAPI stain to delineate the spatial distribution of cells in the biomass sample (Fig. 4A). Fluozin-1 binds to Cd(II), so Fig. 4B illustrates the spatial distribution of Cd in the sample. Comparison of Fig. 4A and B, and examination of the composite of the two (Fig. 4C) indicates that although there is a concentration of Cd at the cells within the biomass, a significant portion of the bound Cd is attached to EPS molecules exterior to the bacterial cells.

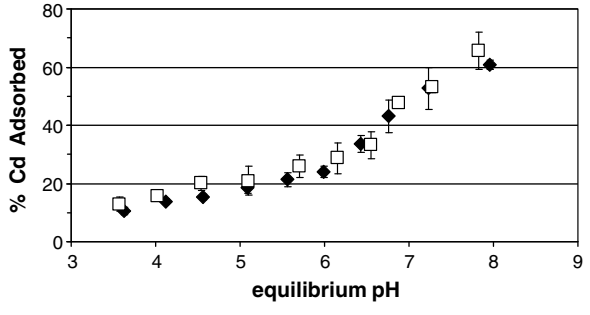

Fig. 3. Cd adsorption data for untreated (EPS-bearing; black diamonds) and enzyme-treated (EPS-free; grey squares) biomass samples in terms of percentage of total Cd that was adsorbed as a function of pH. All experiments contained 1.2 gm biomass (wet mass)/L, 10 ppm Cd, in a 0.1 M $NaClO_4$ electrolyte solution.

3.5. FTIR spectroscopy

FTIR spectra of the untreated and enzyme-treated Cd-free cells are reproducible between spots analyzed and in general are similar to each other. Due to the complexity of the IR spectra for the biomass, characteristic peaks were assigned to main functional groups associated with both the treated and untreated cells. Shown in Fig. 5, and tabulated in Table 2, are representative spectra for the treated and untreated cells. Each spectrum exhibits peaks that likely correspond to Amide I (ν (C═O), ν(C─N), δ(N─H); 1660–1637 cm^{-1}), Amide II (coupling of δ(N─H) and ν(C─N); 1550–1540 cm^{-1}), CH_2 scissoring (~1450 cm^{-1}), carboxyl and phosphoryl vibrations ($\nu_s(COO^-)$ at ~1400; ν_{as}(P═O) at 1240–1220 cm^{-1}) and vibrations associated with phosphate and polysaccharide moieties (~950–1150 cm^{-1}) (Brandenburg and Seydel, 1996; Naumann et al., 1996; Jiang et al., 2004; Parikh and Chorover, 2005; Parikh and Chorover, 2006). The similarity in the spectra between the treated and the untreated cells is not unexpected. Although the composition of the *P. putida* EPS is dominantly alginate-like (Conti et al., 1994), it is likely to contain a number of other components that include carboxyl, phosphoryl, and possibly other binding site types. The FTIR results suggest that the overall composition of binding sites within the EPS may be similar to that of the cell wall in general. Free EPS extracted from *Escherichia coli* MG1655 gave a spectrum similar to those observed here (Eboigbodin and Biggs, 2008).

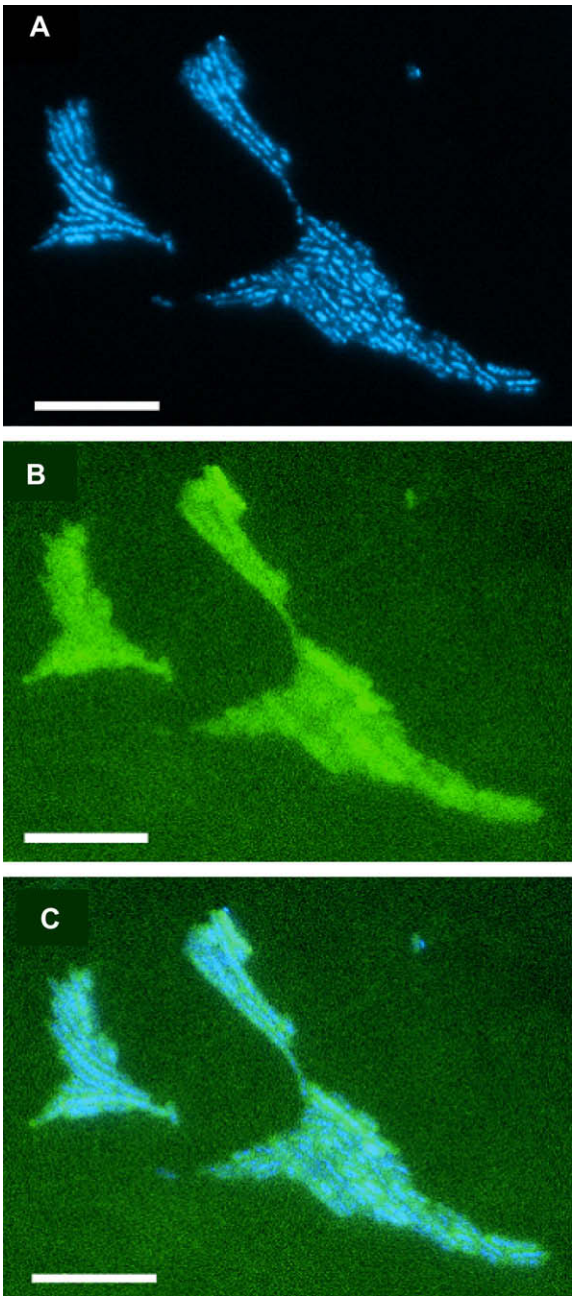

Fig. 4. Fluorescence microscopy images of untreated (EPS-bearing) *P. putida* cells stained with (A) DAPI to delineate cell positions, and (B) Fluozin-1 to indicate location of Cd (lighter shade indicates a higher Cd concentration). (C) represents the composite image of (A) and (B), more clearly demonstrating Cd adsorption exterior to the bacterial cells. Bar: 10 μm.

Exposure of the untreated and enzyme-treated cells to Cd typically resulted only in subtle changes to the FTIR spectra compared to the Cd-free samples. For both untreated and enzyme-treated samples that were exposed to Cd, there was greater variability amongst the ten spectra collected than was observed for the Cd-free biomass samples. The greater variability in the spectra collected suggests greater sample heterogeneity and may indicate preferential binding of Cd to specific sites/localized conditions. Of the ten spots analyzed for Cd-exposed untreated cells, eight spots exhibited similar spectra, represented by spectrum (b) in Fig. 5, and two spots exhibited spectra represented by spectrum (c). Of the ten spots analyzed for Cd-reacted enzyme-treated cells, nine spots exhibited spectra represented by spectrum (e), and one sample spot yielded a different spectrum, shown by spectrum (f).

Functional groups that absorb in the energy region 950–1150 cm^{-1} include the PO_2^- (asymmetric and symmetric stretching), C—OH and C—C groups of alcohols and polysaccharides (Jiang et al., 2004), and C—O—P and C—O—C groups (Eboigbodin and Biggs, 2008). Bands associated with these groups overlap extensively in this region, making peak assignment difficult. Spectra (a) and (d) in Fig. 5 (the treated and untreated Cd-free samples) exhibit a peak at 1087 cm^{-1}, which has been assigned to the P=O stretch. For two of the sampled locations in the untreated sample and for one of the sampled locations in the treated sample, exposure to Cd significantly alters this peak. In the untreated sample, two sampled locations (spectrum (c), Fig. 5) exhibited a peak shift in this region to ~1058 cm^{-1} and a significant broadening of the peak region. In the enzyme-treated sample, this peak shift was not observed with exposure to Cd (spectra (e) and (f), Fig. 5), but a similar peak broadening was observed at one of the sampled locations [spectrum (f)]. These changes suggest that, at these locations, Cd is complexed directly with phosphoryl and polysaccharide groups.

The majority of the Cd-exposed samples did not show the dramatic changes observed in spectra (c) and (f) at 1087 cm^{-1}. However, the presence of Cd did affect the peak shape and intensity between treated and untreated cells (Fig. 6). With these samples, we typically observed a slight shift in position of the band at 1087 cm^{-1} to lower energy. In the untreated and enzyme-treated cells, this band is reproducibly positioned at 1087 cm^{-1} (untreated: 1087.1 ± 1.05 cm^{-1}; enzyme 1087 ± 1.7 cm^{-1}), but is shifted to 1084 (±1.3) cm^{-1} for untreated biomass exposed to Cd, and to 1083 (±1.3 cm^{-1}) for treated biomass exposed to Cd.

Other changes in the FTIR spectra between the unexposed and Cd-exposed cells include a slight broadening and shift of the peak at ~1240 cm^{-1}, as demonstrated in detail in Fig. 6. In other spectroscopic studies of bacteria, this peak has been attributed to vibrations of either phosphate (Jiang et al., 2004) or carboxyl moieties (Leone et al., 2007). Interaction of Cd with the cells may occur in association with both groups (e.g., Boyanov et al., 2003) and it is likely that the observed broadening of the peak at ~1240 cm^{-1} in all biomass reacted with Cd results from such interactions. As demonstrated by spectra (b) and (e), reaction of both the treated and untreated biomass with Cd results in the appearance of a new band at ~1208 cm^{-1}. This shift is likely due to interaction of Cd with PO_2^- groups, as complexation of Cd would weaken the P=O character and shift the absorption to lower energy.

The FTIR results in this study exhibit subtle effects of Cd binding onto both the treated and untreated biomass samples, and only subtle differences that result from the treatment of the biomass and removal of EPS material. The FTIR

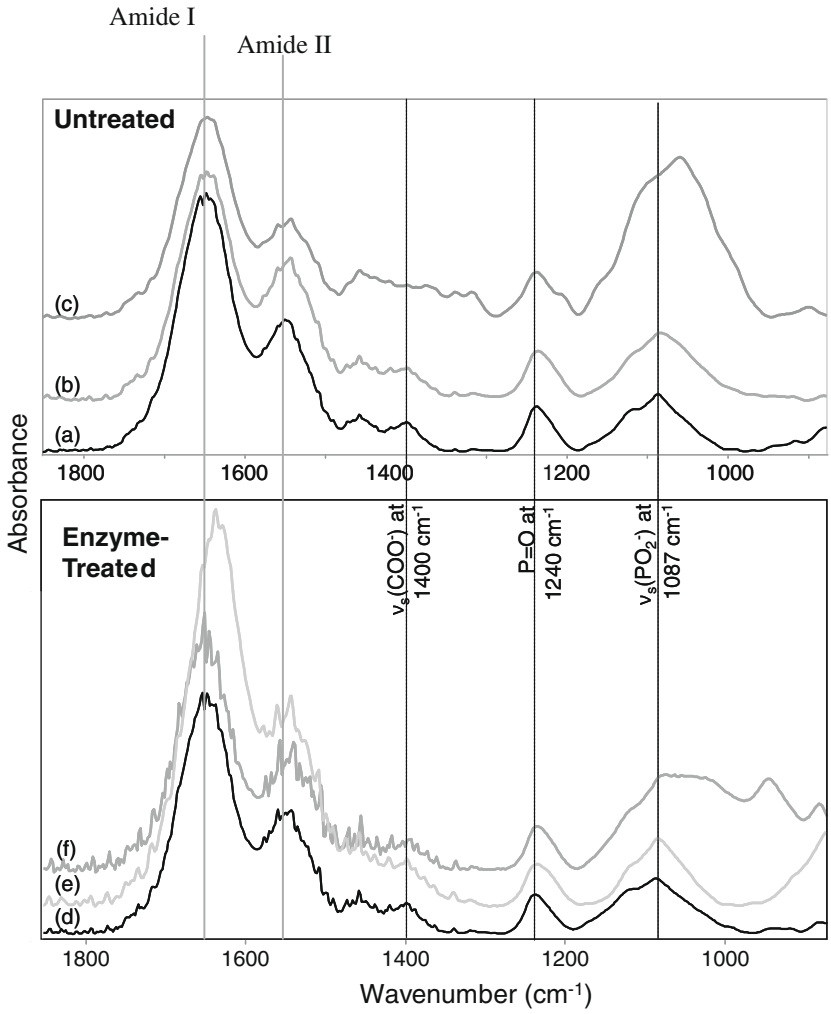

Fig. 5. FTIR spectra of untreated (upper panel) and enzyme-treated (lower panel) biomass before and after exposure to solutions with 50 ppm nominal Cd concentrations. Spectra were taken from 10 spots on the sample. Spectrum (a) is for the untreated cells, and (b) and (c) are representative spectra for untreated cells exposed to Cd. Spectrum (b) was more typical (representing 8 of 10 scans). Spectrum (d) is for the treated cells and (e) and (f) representative spectra for treated cells exposed to Cd. Again, spectrum (e) is more typical (representing 9 of 10 scans). The vertical lines highlight bands important for interpreting functional group interactions with Cd.

Table 2
Absorption bands of functional groups associated with the whole bacterial cells

Absorption bands (cm^{-1})	Vibrational modes
3300–3500	ν(O—H) and ν(N—H)
2900–3000	ν(C—H) of —CH_2 and —CH_3 groups
1637–1660	Amide I (ν(C=O), ν(C=N), δ(N—H))
1540–1550	Amide II (coupling of δ(N—H) and ν(C—N))
1450	CH_2 scissors
1420–1400	ν_s(COO—)
1220–1260	—COOH and C—O—C (esters) vibrations, $\nu_{as}(PO_2^-)$
950–1150	$\nu(PO_2^-)$, ν(P—OH), C—O—C, C—OH and C—C vibrations (polysaccharides and alcohols), ring vibrations
> 1000	Phosphates and sulphur groups (“Fingerprint” zone)

Band assignments are those previously reported for bacteria (e.g. Jiang et al., 2004; Parikh and Chorover, 2005, Kazy et al., 2006; Parikh and Chorover, 2006; Eboigbodin and Biggs, 2008).

results suggest that Cd binding onto the biomass involves either phosphoryl or carboxyl sites, or both. The most significant effects of the enzyme treatment are seen in the region associated with phosphate and polysaccharides vibrations (i.e., between ~900 and ~1200 cm^{-1} in Figs. 5 and 6). The broad peak located in this region is narrower for the enzyme-treated samples compared to the untreated ones. Small shifts in the positions of these peaks between the treated and

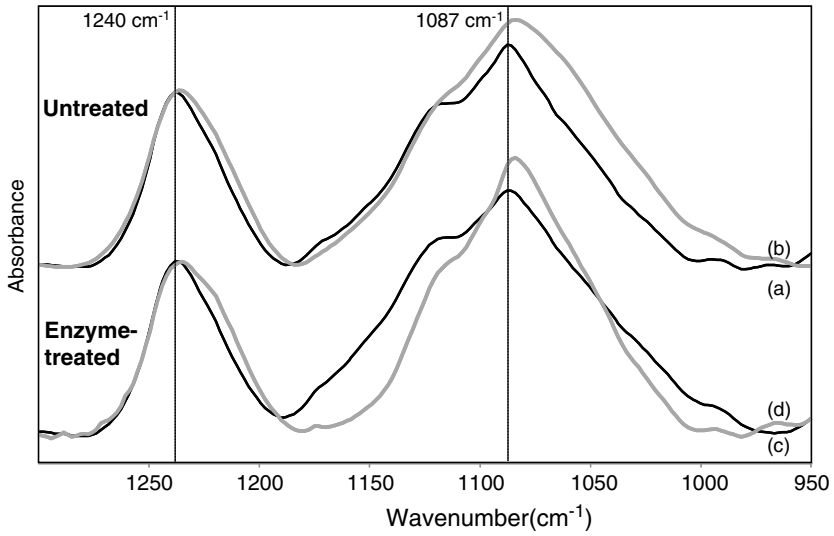

Fig. 6. FTIR spectra in the 950–1300 cm^{-1} region of untreated and treated biomass before and after exposure to solutions with 50 ppm Cd (nominal concentrations). Spectrum (a) is for the untreated cells and (b) is the representative (typical) spectrum for untreated cells exposed to Cd. Spectrum (c) is for the treated cells and (d) is the representative spectrum (typical) for treated cells exposed to Cd. This figure highlights the subtle changes to the FTIR spectrum with Cd binding that was typically observed. The vertical lines highlight bands important for interpreting functional group interactions with Cd.

the untreated samples likely reflect the fact that the enzyme treatment digests specific sugars (polysaccharides with α-1,4-glycosidic bonds) which may bind Cd under pristine conditions (i.e. in the presence of EPS). In general, the FTIR results suggest similar binding environments for Cd in the treated and untreated biomass samples. Although similar, the treated and untreated biomass samples exhibit some subtle, yet significant spectral differences, suggesting that EPS material binds a significant portion of the total Cd adsorbed onto the untreated biomass sample.

3.6. Effect of EPS on cell viability

A possible role of metal binding onto EPS molecules can be seen in the measurements of the effects of EPS on cell viability, as measured by fluorescence microscopy with LIVE/DEAD staining of the biomass (Fig. 7). Treated biomass samples, with the EPS material removed, exhibit a large effect of Cd on the viability of the bacterial cells within the sample. The viability drops from approximately 70% viable cells in the sample that was not exposed to Cd to approximately 30% viable cells in the Cd-exposed sample. The presence of EPS material not only enhances the viability of cells in the sample (with approximately 80% viable cells in the untreated sample not exposed to Cd), but the EPS also serves to minimize the toxic effects of Cd. Cd exposure decreases the viability of the cells in the untreated biomass samples, but not to the extent that we observed for the EPS-free treated sample. The beneficial effect of the EPS is likely due to EPS binding of toxic aqueous Cd, thereby diminishing the activity of Cd to which the cells within the EPS-bearing biomass are exposed.

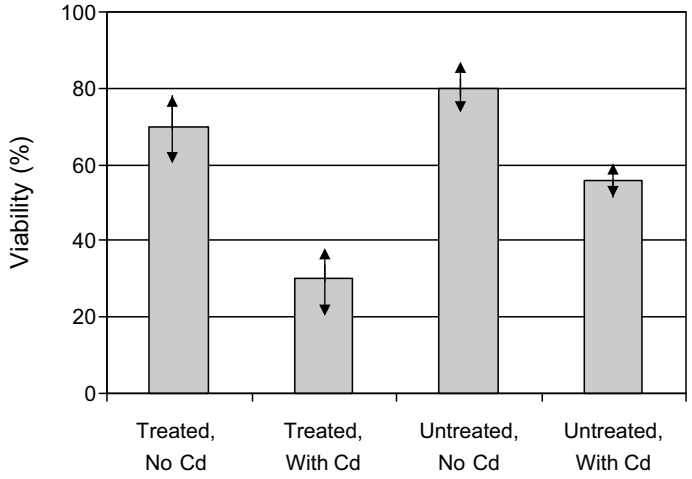

Fig. 7. Viability of untreated and enzyme-treated *P. putida* biomass at pH 6.5 after a 6 h exposure to 0.1 M $NaClO_4$ with or without 10 ppm Cd. Double arrows represent 1 standard deviation associated with each average value.

4. CONCLUSIONS

Both the potentiometric titration experiments and the Cd adsorption experiments indicate that the presence of EPS in a biomass sample does not significantly affect the adsorption reactivity of the biomass on a per mass basis, nor are differences in Cd-binding groups readily apparent with FTIR. These results imply that either the EPS contains no proton or Cd-binding ability, or that it exhibits a binding ability that is essentially identical to that exhibited by bacterial cells alone. However, the fluorescence microscopy and cell viability experiments each suggest that EPS material can bind significant concentrations of Cd from solution. Although the Cd-binding mechanisms of EPS and the cell wall are not well-defined by our data, our results strongly suggest that significant concentrations of Cd (and presumably other aqueous cations) can be bound to EPS material within biofilms, and that the Cd-binding mechanisms are similar for EPS and cell walls, at least for the biomass studied here. Furthermore, because we observe no significant differences on a per mass basis between biomass samples with and without EPS, our results suggest that, if other species behave similar to *P. putida*, metal binding onto EPS-bearing biomass can be modeled successfully using surface complexation modeling parameters that were derived from bacteria-only experimental systems, and that one need not distinguish between EPS binding and bacterial cell wall binding in order to account for metal distributions in biofilm-bearing systems.

ACKNOWLEDGMENTS

Research funding was provided by a National Science Foundation Environmental Molecular Science Institute (EMSI) Grant to the University of Notre Dame (EAR02-21966). Analytical facilities within EMSI and the Center for Environmental Science and Technology at the University of Notre Dame were used in this research. Notre Dame undergrad Maria Mazzillo and Lisa Vukovits, a Research Experience for Teachers participant, conducted some of the experiments. Two anonymous journal reviews and comments by Associate Editor Susan Glasauer significantly improved the presentation of this research.

REFERENCES

Allesen-Holm M., Barken K. B., Yang L., Klausen M., Webb J. S., Kjelleberg S., Molin S., Givskov M. and Tolker-Nielsen T. (2006) A characterization of DNA release in *Pseudomonas aeruginosa* cultures and biofilms. *Mol. Microbiol.* **59**, 1114–1128.

Arroyo L. J., Li F., Teppen B. J., Johnston C. T. and Boyd S. A. (2005) Oxidation of 1-naphthol coupled to reduction of structural Fe^{3+} in smectite. *Clay. Clay Miner.* **53**, 587–596.

Beveridge, T.J. (1988) Wall ultrastructure: how little we know. In *Antibiotic Inhibition of the Bacterial Cell: Surface Assembly and Function* (eds. P. Actor, L. Daneo-Moore, M. L. Higgins, M. R. J. Salton, and G. D. Shockman). Amer. Soc. Microbiol., Washington, DC. pp. 3–20.

Böckelman U., Szewzyk U. and Grohmann E. (2003) A new enzymatic method for the detachment of particle associated soil bacteria. *J. Microbiol. Methods* **55**, 201–211.

Borrok D. M. and Fein J. B. (2005) The impact of ionic strength on the adsorption of protons, Pb, Cd, and Sr onto the surfaces of Gram negative bacteria: testing non-electrostatic, diffuse, and triple layer models. *J. Colloid Interface Sci.* **286**, 110–126.

Borrok D. M., Fein J. B., Tischler M., O'Loughlin E., Meyer H., Liss M. and Kemner K. (2004) The effect of acidic solutions and growth conditions on the adsorptive properties of bacterial surfaces. *Chem. Geol.* **209**, 107–119.

Borrok D., Fein J. B. and Turner B. F. (2005) A universal surface complexation framework for modeling proton binding onto bacterial surfaces in geologic settings. *Am. J. Sci.* **305**, 826–853.

Boyanov M. I., Kelly S. D., Kemner K. M., Bunker B. A., Fein J. B. and Fowle D. A. (2003) Adsorption of cadmium to B. subtilis bacterial cell walls—a pH-dependent XAFS spectroscopy study. *Geochim. Cosmochim. Acta* **67**, 3299–3311.

Brandenburg K. and Seydel U. (1996) Fourier transform infrared spectroscopy of cell surface polysaccharides. In *Infrared Spectroscopy of Biomolecules* (eds. H. H. Mantsch and D. Chapman). Wiley-Liss, New York, pp. 203–238.

Brisou J. F. (1995) *Biofilms: Methods for Enzymatic Release of Microorganisms*. CRC press, Boca Raton, Florida, pp. 204.

Comte S., Guibaud G. and Baudu M. (2006a) Relations between extraction protocols for activated sludge extracellular polymeric substances (EPS) and EPS complexation properties Part I. Comparison of the efficiency of eight EPS extraction methods. *Enzyme Microbial Technol.* **38**, 237–245.

Comte S., Guibaud G. and Baudu M. (2006b) Relations between extraction protocols for activated sludge extracellular polymeric substances (EPS) and complexation properties of Pb and Cd with EPS Part II. Consequences of EPS extraction methods on Pb^{2+} and Cd^{2+} complexation. *Enzyme Microbial Technol.* **38**, 237–245.

Conti E., Flaibani A., O'Regan M. and Sutherland I. W. (1994) Alginate from *Pseudomonas fluorescens* and *P. putida*: production and properties. *Microbiology* **140**, 1125–1132.

Costerton J. W., Lewandowski Z., Caldwell D. E., Korber D. R. and Lappinscott H. M. (1995) Microbial biofilms. *Annu. Rev. Microbiol.* **49**, 711–745.

Davey M. E. and O'Toole G. A. (2000) Microbial biofilms: from ecology to molecular genetics. *Microbiol. Mol. Biol. Rev.* **64**, 847–867.

Eboigbodin K. E. and Biggs C. A. (2008) Characterization of the extracellular polymeric substances produced by *Escherichia coli* using infrared spectroscopic, proteomic, and aggregation studies. *Biomacromolecules* **9**, 686–695.

Fein J. B., Boily J.-F., Yee N., Gorman-Lewis D. and Turner B. F. (2005) Potentiometric titrations of *Bacillus subtilis* cells to low pH and a comparison of modeling approaches. *Geochim. Cosmochim. Acta* **69**, 1123–1132.

Ferris F. G., Schultze S., Witten T. C., Fyfe W. S. and Beveridge T. J. (1989) Metal interactions with microbial biofilms in acidic and neutral pH environments. *Appl. Environ. Microbiol.* **55**, 1249–1257.

Flemming H. C. and Wingender J. (2001) Relevance of microbial extracellular polymeric substances (EPSs): Part I. Structural and ecological aspects. *Water Sci. Technol.* **43**, 1–8.

Foster L. J. R., Moy Y. P. and Rogers P. L. (2000) Metal binding capabilities of *Rhizobium etli* and its extracellular polymeric substances. *Biotechnol. Lett.* **22**, 1757–1760.

Fowle D. A. and Fein J. B. (2000) Experimental measurements of the reversibility of metal-bacteria adsorption reactions. *Chem. Geol.* **168**, 27–36.

Geesey G. G. and Jang L. (1990) Extracellular polymers for metal binding. In *Microbial Mineral Recovery* (eds. H. L. Ehrlich and C. L. Brierley). McGraw-Hill Book Co., New York, pp. 223–247.

Guibaud G., van Hullebusch E. and Bordas F. (2006) Lead and cadmium biosorption by extracellular polymeric substances (EPS) extracted from activated sludges: pH-sorption edge tests and mathematical equilibrium modelling. *Chemosphere* **64**, 1955–1962.

Guine V., Spadini L., Sarret G., Muris M., Delolme C., Gaudet J.-P. and Martins J. M. F. (2006) Zinc sorption to three gram-negative bacteria: combined titration, modeling, and EXAFS study. *Environ. Sci. Technol.* **40**, 1806–1813.

Jiang W., Saxena A., Song B., Ward B., Beveridge T. J. and Myneni S. C. B. (2004) Elucidation of functional groups on Gram-positive and Gram-negative bacterial surfaces using infrared spectroscopy. *Langmuir* **20**, 11433–11442.

Kazy S. K., Das S. K. and Sar P. (2006) Lanthanum biosorption by a *Pseudomonas* sp.: equilibrium studies and chemical characterization. *J. Ind. Microbiol. Biotech* **33**, 773–783.

Lau T. C., Wu X. A., Chua H., Qian P. Y. and Wong P. K. (2005) Effect of exopolysaccharides on the adsorption of metal ions by *Pseudomonas* sp. CU-1. *Water Sci. Technol.* **52**, 63–68.

Leone L., Ferri D., Manfredi C., Persson P., Shchukarev A., Sjöberg S. and Loring J. (2007) Modelling the acid–base properties of bacterial surfaces: a combined spectroscopic and potentiometric study of the Gram positive bacterium *Bacillus subtilis*. *Environ. Sci. Technol.* **41**, 6465–6471.

Liu H. and Fang H. H. P. (2002) Characterization of electrostatic binding sites of extracellular polymers by linear programming analysis of titration data. *Biotechnol. Bioeng.* **80**, 806–811.

McLean R. J. C., Beauchemin D., Clapham L. and Beveridge T. J. (1990) Metal-binding characteristics of the gamma-glutamyl capsular polymer of *Bacillus licheniformis* ATCC 9945. *Appl. Environ. Microbiol.* **56**, 3671–3677.

Mittelman M. W. and Geesey G. G. (1985) Copper-binding characteristics of exopolymers from a freshwater sediment bacterium. *Appl. Environ. Microbiol.* **49**, 846–851.

Naumann D., Schultz C. P. and Helm D. (1996) What can infrared spectroscopy tell us about the structure and composition of intact bacterial cells? In *Infrared Spectroscopy of Biomolecules* (eds. H. H. Mantsch and D. Chapman). Wiley-Liss, New York, pp. 279–310.

Parikh S. J. and Chorover J. (2005) FTIR spectroscopic study of biogenic Mn-oxide formation by *Pseudomonas putida* GB-1. *Geomicrobiol. J.* **22**, 207–218.

Parikh S. J. and Chorover J. (2006) ATR-FTIR spectroscopy reveals bond formation during bacterial adhesion to iron oxide. *Langmuir* **22**, 8492–8500.

Sutherland I. W. (1995) Polysaccharide lyases. *FEMS Microbial. Rev.* **16**, 323–347.

Templeton A. S., Trainor T. P., Traina S. J., Spormann A. M. and Brown, Jr., G. E. (2001) Pb(II) distributions at biofilm-metal oxide interfaces. *Proc. Natl. Acad. Sci.* **98**, 11897–11902.

Templeton A. S., Spormann A. M. and Brown G. E. (2003) Speciation of Pb(II) sorbed by *Burkholderia cepacia*/goethite composites. *Environ. Sci. Technol.* **37**, 2166–2172.

Toner B., Manceau A., Marcus M. A., Millet D. B. and Sposito G. (2005) Zinc sorption by a bacterial biofilm. *Environ. Sci. Technol.* **39**, 8288–8294.

Tourney J., Ngwenya B. T., Mosselmans J. W. F., Tetley L. and Cowie G. L. (2008) The effect of extracellular polymers (EPS) on the proton adsorption characteristics of the thermophile *Bacillus licheniformis* S-86. *Chem. Geol.* **247**, 1–15.

Vincent P., Pignet P., Talmont F., Bozzi L., Fournet B., Guezennec J., Jeanthon C. and Prieur D. (1994) Production and characterization of an exopolysaccharide excreted by a deep-sea hydrothermal vent bacterium isolated from the polychaete annelid *Alvinella-pompejana*. *Appl. Environ. Microbiol.* **60**, 4134–4141.

Westall J. C. (1982) FITEQL, A computer program for determination of chemical equilibrium constants from experimental data. Version 2.0. Report 82-02, Dept. Chem., Oregon St. Univ., Corvallis, OR, USA.

Xu W., Johnston C. T., Parker P. and Agnew S. F. (2000) Infrared study of water sorption on Na-, Li-, Ca- and Mg-exchanged (SWy-1 and SAz-1) montmorillonite. *Clay. Clay Miner.* **48**, 120–131.

Zherebtsov N. A., Ruadze I. D. and Yakovlev A. N. (1995) Mechanism of acid-catalyzed and enzymatic hydrolysis of starch. *Appl. Biochem. Microbiol.* **31**, 511–514.

Associate editor: Susan Glasauer